DOI: 10.3969/j.issn.1673-3185.2017.06.015 **http:** // english.ship-research.com

Translated from: ZHAO J X, YU X, CHAI K, et al. Vibration isolation performance analysis of double layer vibration isolation system[J]. Chinese Journal of Ship Research, 2017, 12(6): 101-107.

Vibration isolation performance analysis of double-layer vibration isolation system

ZHAO Jianxue[1], *YU Xiang*[2], *CHAI Kai*[1], *YANG Qingchao*[2]

1 College of Power Engineering, Naval University of Engineering, Wuhan 430033, China

2 Office of Research and Development, Naval University of Engineering, Wuhan 430033, China

Abstract: [Objectives] Studying the influence of the system parameters of a quasi-zero-stiffness isolator on vibration isolation performance can provide a key direction for the application of quasi-zero-stiffness isolation in vibration isolation systems. **[Methods]** Based on a double-layer vibration isolation system consisting of linear isolation and quasi-zero-stiffness isolation, as well as an equivalent linear vibration isolation system with two degrees of freedom, dynamic models are separately established. Moreover, the averaging method is applied to derive the power transfer rates under the conditions of two harmonic-force excitation systems. It is proven that the double-layer vibration isolation system has better vibration isolation performance than the equivalent linear vibration isolation system with two degrees of freedom, and a method for enhancing the vibration isolation effect of the double-layer vibration isolation system is proposed. **[Results]** The results show that the power transfer rate of the double-layer vibration isolation system is less than 1 at the second order resonance frequency, which means that it has the effect of vibration isolation in the vicinity of the resonance frequency of the second order, which overcomes the shortcomings of the linear vibration isolation system with two degrees of freedom. **[Conclusions]** The double-layer vibration isolation system can improve vibration isolation performance by appropriately reducing the damping ratio, mass ratio and stiffness ratio, giving it better low-frequency vibration isolation performance than the equivalent linear vibration isolation system.

Key words: quasi-zero stiffness; double-layer vibration isolation; power transfer rate

CLC number: U661.44; O322

0 Introduction

According to traditional theories of vibration isolation, the initial vibration isolation frequency of a linear vibration isolator is $\sqrt{2}$ times the natural frequency of the system. In order to realize low-frequency vibration isolation, it is necessary to reduce the stiffness of the linear vibration isolator, but the bearing capacity of the system will be weakened as a result. Thus, scholars all over the world have proposed to use quasi-zero-stiffness vibration isolators with higher static stiffness and lower dynamic stiffness[1], which can overcome the contradiction between reducing the natural frequency of a linear vibration isolator and increasing its bearing capacity, with good effect of low-frequency vibration isolation[2-3], showing a broad application prospect in the field of vibration and noise control of ship power equipment. Compared with linear vibration isolators, quasi-zero-stiffness ones perform better in low-frequency vibration isolation and generate wider frequency bands of vibration isolation, when they are used for double-layer vibration isolation and floating-raft vibration isolation[4-5]. For example, Wang et al.[4] established a piecewise nonlinear dynamic model of a quasi-zero-stiffness double-layer vibration isolation system with rollers, and evaluated the system performance in vibration isolation; relevant results showed that

Received: 2017-03-20

Supported by: National Natural Science Foundation of China (51679245); Young Scientists Fund of the National Natural Science Foundation of China (51509253)

Author(s): ZHAO Jianxue (Corresponding author), male, born in 1992, master candidate. Research interest: vibration and noise control. E-mail: 916082120@qq.com

YU Xiang, male, born in 1978, Ph.D., senior engineer. Research interest: vibration and noise control. E-mail: yuxiang898@sina.com

the quasi-zero-stiffness double-layer vibration isolation system not only performed well in low-frequency vibration isolation, but also had wider frequency bands of vibration isolation. Zhou et al.[5] constructed a quasi-zero-stiffness single-layer vibration isolation floating raft by using quasi-zero-stiffness vibration isolators, and evaluated the system performance in vibration isolation; relevant results showed that the initial frequency of the quasi-zero-stiffness floating-raft vibration isolation was much lower than that of the linear floating-raft vibration isolation, and that the system had much higher vibration isolation efficiency than a linear system did.

Evaluation indexes of performance of vibration isolation systems mainly include: vibration level differences, power transfer rates (insertion loss), force transfer rates, and transmitted power flow. As for vibration isolation systems installed on flexible foundations, due to differences in amplitudes and phases of transfer force at multiple supports, methods for evaluating vibration isolation effects in terms of power transfer rates or response ratios show certain defects, but power transfer rates are more accurate and comprehensive than both transmitted power flow and vibration level differences in evaluating the vibration isolation performance of systems[6]. Therefore, more and more attention has been paid to methods using power transfer rates in recent years. Lou et al.[7] simplified a foundation into an elastic beam with two fixed ends, derived the transmitted power flow of a single-layer flexible vibration isolation system through the method of mechanical impedance, analyzed the influences of off-center excitation on the characteristics of the power transfer by means of numerical simulation, and compared the power flow with the spectrum curves of vibration level difference. Xia et al.[8] simulated a flexible foundation by using a rectangular damping sheet with four simply-supported edges, obtained formulas of the power transfer in the vibration isolation system through the method of mechanical impedance, and discussed the influences of various system parameters on the vibration isolation effect. As the vibration isolation effect of a quasi-zero-stiffness vibration isolation system will be affected by system parameters, research on the influences of the system parameters on vibration isolation performance can provide guidance for the application of quasi-zero-stiffness vibration isolators to vibration isolation systems.

In this paper, dynamic models of a double-layer vibration isolation system, composed of linear vibration isolation and quasi-zero-stiffness vibration isolation, and a linear vibration isolation system with two degrees of freedom were established respectively; according to the definition of power transfer rates, the method of averaging was adopted to derive power transfer rates of the two systems under harmonic-force excitation; influences of parameters such as the amplitude of excitation force, damping ratio, mass ratio, and stiffness ratio on the power transfer rate and the resonance frequency of the double-layer vibration isolation system were analyzed numerically, so as to propose methods for improving the vibration isolation performance of the double-layer vibration isolation system; in addition, power transfer rates of the two systems were compared and analyzed.

1 Establishment of dynamic models and solutions for power transfer rates

1.1 Model of a quasi-zero-stiffness vibration isolator

As shown in Fig.1, the quasi-zero-stiffness vibration isolator is composed of a vertical spring with positive stiffness and two inclined springs with negative stiffness[9]. In the figure, k_0 and k_1 respectively denote stiffness of the inclined and vertical springs in the quasi-zero-stiffness vibration isolator; L_0 denotes the length of either inclined spring; h indicates the compression amount of the vertical spring when the system is in balance; a indicates the distance from the installation position of either inclined spring to the center of the system; and x indicates displacement of the vibration isolator.

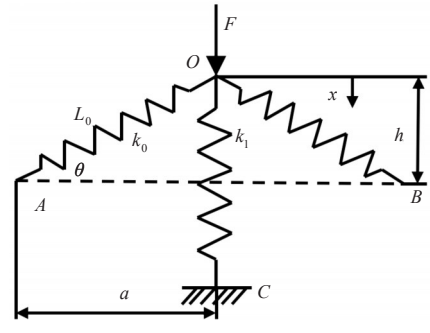

Fig.1 Schematic diagram of quasi-zero stiffness isolator

In the case of external force F acting on the system, the vertical force of the two inclined springs with negative stiffness is:

$$f_0 = 2k_0(h-x)\left(\frac{L_0}{\sqrt{a^2+(h-x)^2}}-1\right) \quad (1)$$

Under the action of the external force F, the force of the quasi-zero-stiffness system in the vertical direction is:

$$F_{\mathrm{V}} = k_1 x + f_0 \tag{2}$$

Substituting f_0 into Formula (2) yields:

$$F_{\mathrm{V}} = k_1 x + 2k_0(x-h)\left(1 - \frac{L_0}{\sqrt{a^2 + (x-h)^2}}\right) \tag{3}$$

Non-dimensionalizing Formula (3) yields:

$$F_{\mathrm{V}}^{*} = \hat{y} + 2\beta\hat{y}\left(1 - \frac{1}{\sqrt{a'^2 + \hat{y}^2}}\right) \tag{4}$$

where $y = x - h$, $\hat{y} = y/L_0$, $a' = a/L_0$, $\beta = k_0/k_1$, $F_{\mathrm{V}}^{*} = \hat{F}_{\mathrm{V}} - \hat{h}$.

By taking a derivative with respect to $\hat{y}$, the dimensionless stiffness of the system can be obtained as:

$$\hat{K} = 1 + 2\beta\left[1 - \frac{a'^2}{\left(\hat{y}^2 + a'^2\right)^{3/2}}\right] \tag{5}$$

Setting $\hat{y} = 0$ and $\hat{K} = 0$ yields the condition for obtaining the quasi-zero stiffness of the system:

$$\beta = \frac{a'}{2(1-a')} \tag{6}$$

From Formula (6), it can be seen that the condition for the system to achieve quasi-zero stiffness is related to the ratio β of the stiffness of vertical spring to the stiffness of inclined springs, the original length L_0 of inclined springs, and the distance a from the installation position of either inclined spring to the center of the system.

Processing Formula (4) through Taylor expansion in the vicinity of the static equilibrium position yields:

$$F_{\mathrm{V}}^{*} = F_{\mathrm{V}}^{*}(0) + F_{\mathrm{V}}^{*}(0)\hat{y} + \frac{F_{\mathrm{V}}^{*}(0)}{2!}\hat{y}^2 + \frac{F_{\mathrm{V}}^{*}(0)}{3!}\hat{y}^3 = \frac{2\beta}{a^{13}}\hat{y}^3$$

Substituting dimensionless parameters into the above formula yields:

$$F_{\mathrm{V}} = \frac{2K_0L_0}{a^3}y^3$$

and thus, the stiffness of the quasi-zero-stiffness vibration isolator is

$$k_{\mathrm{qzs}} = \frac{2K_0L_0}{a^3}$$

1.2 Double-layer vibration isolation system

A double-layer vibration isolation system was established based on the assumption that the foundation was rigid, as shown in Fig.2, in which, the upper layer was a quasi-zero-stiffness vibration isolator and the lower layer was a linear vibration isolator. In the figure: k_{qzs} and k_2 respectively indicate nonlinear stiffness of the quasi-zero-stiffness vibration isolator and stiffness of the linear vibration isolator; c_1 and c_2 respectively indicate damping of the quasi-zero-stiffness vibration isolator and that of the linear vibration isolator; Y_1 and Y_2 respectively indicate displacement of the isolated equipment and that of the intermediate mass block; m_1 and m_2 respectively indicate mass of the isolated equipment and that of the intermediate mass block; $F\cos\Omega T$ indicates the excitation imposed on the isolated equipment.

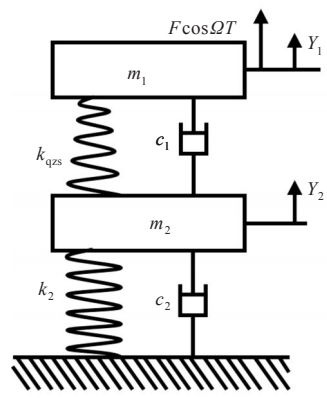

Fig.2 Schematic diagram of double layer vibration isolation system

The upward direction is defined as the positive direction, and the following formula can be obtained according to Fig.2:

$$\begin{cases} m_1\ddot{Y}_1 = k_{\mathrm{qzs}}(Y_2 - Y_1)^3 + c_1(\dot{Y}_2 - \dot{Y}_1) + F\cos\Omega T \\ m_2\ddot{Y}_2 = -k_{\mathrm{qzs}}(Y_2 - Y_1)^3 - c_1(\dot{Y}_2 - \dot{Y}_1) - k_2Y_2 - c_2\dot{Y}_2 \end{cases} \tag{7}$$

Set

$$x_1 = Y_1/a',\ x_2 = Y_2/a',\ t = T\Omega_0,\ \omega = \frac{\Omega}{\Omega_0},$$

$$\Omega_0 = \sqrt{\frac{k_1}{m_1}},\ \xi_1 = \frac{c_1\Omega_0}{k_1},\ f = \frac{F}{k_1a},\ k_{\mathrm{qzs}} = \frac{2K_0L_0}{a^3},$$

$$\beta = \frac{k_0}{k_1},\ \xi_1 = \frac{c_2\Omega_0}{k_1},\ \gamma = \frac{2\beta+1}{6},\ w = \frac{m_1}{m_2} \tag{8}$$

where a refers to the distance from the left installation point of the negative-stiffness mechanism to the center of the quasi-zero-stiffness vibration isolator, as mentioned in Section 1.1. Thus, Formula (7) can be transformed into a dimensionless nonlinear system model:

$$\begin{cases} \ddot{x}_1 = \gamma(x_2 - x_1)^3 + \xi_1(\dot{x}_2 - \dot{x}_1) + f\cos\omega t \\ \ddot{x}_2 = -w\gamma(x_2 - x_1)^3 - w\xi_1(\dot{x}_2 - \dot{x}_1) - w\lambda x_2 - w\xi_2\dot{x}_2 \end{cases} \tag{9}$$

Set $z_1 = x_2 - x_1$, $z_2 = x_2$ Formula (9) can be transformed into:

$$\begin{cases}\ddot{z}_1-\ddot{z}_2+\gamma z_1^3+\xi_1\dot{z}_1+f\cos\omega t=0\\ w\ddot{z}_1-(1+w)\ddot{z}_2-w\lambda z_2-w\xi_2\dot{z}_2+wf\cos\omega t=0\end{cases} \tag{10}$$

In the form of matrices, Formula (10) can be transformed into:

$$\boldsymbol{M}\ddot{\boldsymbol{Z}}+\boldsymbol{C}\dot{\boldsymbol{Z}}=\hat{\boldsymbol{f}} \tag{11}$$

where

$$\boldsymbol{Z}=\begin{bmatrix}z_1\\ z_2\end{bmatrix},\ \boldsymbol{M}=\begin{bmatrix}1 & -1\\ w & -(1+w)\end{bmatrix},$$

$$\hat{\boldsymbol{f}}=\begin{bmatrix}-f\cos\omega t-\gamma z_1^3\\ -wf\cos\omega t+w\lambda z_2\end{bmatrix},\ \boldsymbol{C}=\begin{bmatrix}\xi_1 & 0\\ 0 & -w\xi_2\end{bmatrix}$$

With the method of averaging [9], it is supposed that solutions to steady-state responses of the system are:

$$\boldsymbol{Z}=\boldsymbol{u}\cos\omega t+\boldsymbol{v}\sin\omega t \tag{12}$$

$$\dot{\boldsymbol{Z}}=-\omega\boldsymbol{u}\sin\omega t+\omega\boldsymbol{v}\cos\omega t \tag{13}$$

where $\boldsymbol{u}=[u_1,u_2]^{\mathrm{T}}$ and $\boldsymbol{v}=[v_1,v_2]^{\mathrm{T}}$ are slowly varying functions with respect to time t. Taking derivatives of Formula (12) with respect to time t yields:

$$\dot{\boldsymbol{Z}}=\dot{\boldsymbol{u}}\cos\omega t-\omega\boldsymbol{u}\sin\omega t+\dot{\boldsymbol{v}}\sin\omega t+\omega\boldsymbol{v}\cos\omega t \tag{14}$$

$$\ddot{\boldsymbol{Z}}=-\omega\dot{\boldsymbol{u}}\sin\omega t-\omega^2\boldsymbol{u}\cos\omega t+\omega\dot{\boldsymbol{v}}\cos\omega t-\omega^2\boldsymbol{v}\sin\omega t \tag{15}$$

Combining Formula (13) with Formula (14) yields:

$$\dot{\boldsymbol{u}}\cos\omega t+\dot{\boldsymbol{v}}\sin\omega t=0 \tag{16}$$

Substituting Formula (12), Formula (13) and Formula (15) into Formula (11) yields:

$$(\boldsymbol{M}\omega\dot{\boldsymbol{v}}-\boldsymbol{M}\omega^2\boldsymbol{u}+\boldsymbol{C}\omega\boldsymbol{v})\cos\omega t-(\boldsymbol{M}\omega\dot{\boldsymbol{u}}+\boldsymbol{M}\omega^2\boldsymbol{v}+\boldsymbol{C}\omega\boldsymbol{u})\sin\omega t=\hat{\boldsymbol{f}} \tag{17}$$

Combining Formula (16) with Formula (17) yields:

$$\boldsymbol{M}\omega\dot{\boldsymbol{u}}=-(\boldsymbol{M}\omega^2\boldsymbol{v}+\boldsymbol{C}\omega\boldsymbol{u})\sin^2\omega t-\hat{\boldsymbol{f}}\sin\omega t+(-\boldsymbol{M}\omega^2\boldsymbol{u}+\boldsymbol{C}\omega\boldsymbol{v})\cos\omega t\sin\omega t \tag{18}$$

$$\boldsymbol{M}\omega\dot{\boldsymbol{v}}=(\boldsymbol{M}\omega^2\boldsymbol{u}-\boldsymbol{C}\omega\boldsymbol{v})\cos^2\omega t+\hat{\boldsymbol{f}}\cos\omega t+(\boldsymbol{M}\omega^2\boldsymbol{v}+\boldsymbol{C}\omega\boldsymbol{u})\cos\omega t\sin\omega t \tag{19}$$

Terms on the right sides of Formula (18) and Formula (19) can be approximately replaced by using the average of ωt in a cycle, and $\boldsymbol{u}$ and $\boldsymbol{v}$ are deemed to be unchanged within the cycle of ωt. Thus, averaging formulas are given as:

$$\boldsymbol{M}\omega\dot{\boldsymbol{u}}=\frac{1}{2\pi}\int_0^{2\pi}\begin{bmatrix}-\hat{\boldsymbol{f}}\sin\omega t-(\boldsymbol{M}\omega^2\boldsymbol{v}+\boldsymbol{C}\omega\boldsymbol{u})\sin^2\omega t+\\ (-\boldsymbol{M}\omega^2\boldsymbol{u}+\boldsymbol{C}\omega\boldsymbol{v})\cos\omega t\sin\omega t\end{bmatrix}\mathrm{d}\omega t \tag{20}$$

$$\boldsymbol{M}\omega\dot{\boldsymbol{v}}=\frac{1}{2\pi}\int_0^{2\pi}\begin{bmatrix}\hat{\boldsymbol{f}}\cos\omega t+(\boldsymbol{M}\omega^2\boldsymbol{u}-\boldsymbol{C}\omega\boldsymbol{v})\cos^2\omega t+\\ (\boldsymbol{M}\omega^2\boldsymbol{v}+\boldsymbol{C}\omega\boldsymbol{u})\sin\omega t\cos\omega t\end{bmatrix}\mathrm{d}\omega t \tag{21}$$

Formula (20) and Formula (21) can be simplified into:

$$\boldsymbol{M}\omega\dot{\boldsymbol{u}}=-\frac{1}{2}(\boldsymbol{M}\omega^2\boldsymbol{v}+\boldsymbol{C}\omega\boldsymbol{u})+\frac{1}{2}\begin{bmatrix}Q_1\\ Q_2\end{bmatrix} \tag{22}$$

$$\boldsymbol{M}\omega\dot{\boldsymbol{v}}=\frac{1}{2}(\boldsymbol{M}\omega^2\boldsymbol{u}-\boldsymbol{C}\omega\boldsymbol{v})-\frac{1}{2}\begin{bmatrix}Q_3\\ Q_4\end{bmatrix} \tag{23}$$

where

$$Q_1=\frac{3}{4}\gamma v_1^3+\frac{3}{4}\gamma u_1^2v_1,\ Q_2=-w\lambda v_2$$

$$Q_3=\frac{3}{4}\gamma u_1^3+\frac{3}{4}\gamma v_1^2u_1+f,\ Q_4=-w\lambda u_2+wf$$

Terms on the left sides of Formula (22) and Formula (23) are set to be 0, and then solutions to steady-state responses of the system can be expressed by using following polynomials containing v_1, v_2, u_1 and u_2.

$$\omega^2v_1-\omega^2v_2+\xi_1\omega u_1-Q_1=0 \tag{24}$$

$$\omega^2wv_1-\omega^2(1+w)v_2-\omega w\xi_2u_2-Q_2=0 \tag{25}$$

$$-\xi_1\omega v_1+\omega^2u_1-\omega^2u_2-Q_3=0 \tag{26}$$

$$\omega w\xi_2v_2+\omega^2wu_1-\omega^2(1+w)u_2-Q_4=0 \tag{27}$$

When the system is under harmonic-force excitation of $F\cos\Omega T$, the dimensionless force transferred to the intermediate mass block is:

$$f_{\mathrm{t}}=-w\xi_2\dot{z}_2-w\lambda z_2 \tag{28}$$

Substituting Formula (12) and Formula (13) into Formula (28) yields:

$$f_{\mathrm{t}}=F_{\mathrm{t}1}\cos\omega t+F_{\mathrm{t}2}\sin\omega t \tag{29}$$

where

$$F_{\mathrm{t}1}=-w\xi_2\omega v_2-w\lambda u_2,\ F_{\mathrm{t}2}=w\xi_2\omega u_2-w\lambda v_2$$

Then, the amplitude, F_{t} of the dimensionless force, f_{t} transferred to the intermediate mass block can be expressed as:

$$F_{\mathrm{t}}=\sqrt{F_{\mathrm{t}1}^2+F_{\mathrm{t}2}^2} \tag{30}$$

According to Formula (13), the amplitudes of respective dimensionless speeds $\dot{z}_1$, $\dot{z}_2$ of the isolated equipment and the intermediate mass block are:

$$\dot{z}_{\mathrm{t}1}=\sqrt{(-\omega u_1)^2+(-\omega v_1)^2}$$

$$\dot{z}_{\mathrm{t}2}=\sqrt{(-\omega u_2)^2+(-\omega v_2)^2}$$

According to the definition of power transfer rates [10], the power transfer rate of the double-layer vibration isolation system is:

$$T_{\mathrm{p}}=\frac{F_{\mathrm{t}}\dot{z}_{2\mathrm{t}}}{f\dot{z}_{1\mathrm{t}}}=\frac{\sqrt{(w\xi_2\omega u_2-w\lambda v_2)^2+(-w\xi_2\omega v_2-w\lambda u_2)^2}}{f\sqrt{(u_1^2+v_1^2)/(u_2^2+v_2^2)}} \tag{31}$$

1.3 Two-degree-of-freedom linear vibration isolation system

A two-degree-of-freedom linear vibration isolation system was established based on the assumption that the foundation was rigid, as shown in Fig.3. k_1 and k_2 respectively denote the stiffness of the upper and lower vibration isolators; c_1 and c_2 respectively denote the damping of upper and lower vibration isolators; Y_1 and Y_2 respectively denote displacements of the isolated equipment and the intermediate mass

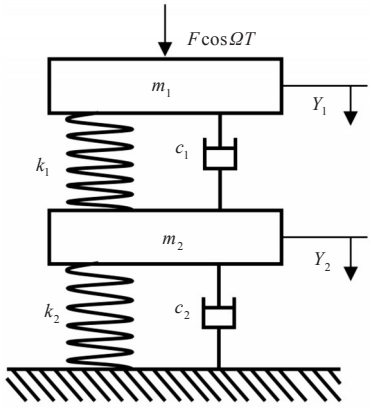

Fig.3 Schematic diagram of two degree of freedom linear vibration isolation system

block; m_1 and m_2 respectively denote mass of the isolated equipment and the intermediate mass block; $F\cos\Omega T$ denotes excitation imposed on the isolated equipment. It is supposed that the spring k_1 has an outer radius of r.

The downward direction is defined as the positive direction, and the following formula can be obtained according to Fig. 3:

$$\begin{cases} m_1\ddot{Y}_1 = -c_1(\dot{Y}_1 - \dot{Y}_2) - k_1(Y_1 - Y_2) + F\cos\Omega T \\ m_1\ddot{Y}_1 = -m_2\ddot{Y}_2 - c_2\dot{Y}_2 - k_2Y_2 + F\cos\Omega T \end{cases} \quad (32)$$

Set $\hat{z}_1 = Y_1 - y_2$, $\hat{z}_2 = Y_2$ and introduce following dimensionless parameters:

$$\Omega_0 = \sqrt{\frac{k_1}{m_1}},\ t = \Omega_0 T,\ \omega = \frac{\Omega}{\Omega_0},\ z_1 = \frac{\hat{z}_1}{r}$$
$$z_2 = \frac{\hat{z}_2}{r},\ \eta_1 = \frac{c_1}{2\sqrt{m_1k_1}},\ \eta_2 = \frac{c_2}{2m_2\Omega_0},$$
$$\lambda = \frac{k_2}{k_1},\ w' = \frac{m_2}{m_1},\ p = \frac{F}{k_1r} \quad (33)$$

Then, dimensionless differential equations of motion of the system are obtained as:

$$\begin{cases} \ddot{z}_1 + \ddot{z}_2 + 2\eta_1\dot{z}_1 + z_1 = p\cos\omega t \\ \ddot{z}_1 + (1+w')\ddot{z}_2 + 2w'\eta_2\dot{z}_2 + \lambda z_2 = p\cos\omega t \end{cases} \quad (34)$$

In the form of matrices, Formula (34) can be expressed as:

$$\boldsymbol{M}\ddot{\boldsymbol{Z}} + \boldsymbol{C}\dot{\boldsymbol{Z}} = \hat{\boldsymbol{f}}_1 \quad (35)$$

where

$$\boldsymbol{Z} = \begin{bmatrix} z_1 \\ z_2 \end{bmatrix},\ \boldsymbol{M} = \begin{bmatrix} 1 & 1 \\ 1 & 1+w' \end{bmatrix},$$
$$\boldsymbol{C} = \begin{bmatrix} 2\eta_1 & 0 \\ 0 & 2w'\eta_2 \end{bmatrix},\ \hat{\boldsymbol{f}}_1 = \begin{bmatrix} p\cos\omega t - z_1 \\ p\cos\omega t + \lambda z_2 \end{bmatrix}$$

By following the same steps as mentioned in Section 1.2, solutions to steady-state responses of the system can be expressed with the following polynomials containing v_1, v_2, u_1 and u_2.

$$\omega^2 v_1 + \omega^2 v_2 + 2\partial_1\omega u_1 - Q_1 = 0 \quad (36)$$
$$\omega^2 v_1 + \omega^2(1+w')v_2 + 2w'\omega\eta_2 u_2 - Q_2 = 0 \quad (37)$$
$$-2\eta_1\omega v_1 + \omega^2 u_1 + \omega^2 u_2 - Q_3 + p = 0 \quad (38)$$
$$-2w'\omega\eta_2 v_2 + \omega^2 u_1 + \omega^2(1+w')u_2 - Q_4 + p = 0 \quad (39)$$

where

$$Q_1 = \frac{3}{4}v_1,\ Q_2 = \lambda v_2,\ Q_3 = u_1,\ Q_4 = \lambda u_2$$

In the case of the system under harmonic-force excitation $F\cos\Omega T$, the dimensionless force transferred to the intermediate mass block is:

$$f_t = 2w'\eta_2\dot{z}_2 + \lambda z_2 \quad (40)$$

The solution is:

$$f_t = F_{t1}\cos\omega t + F_{t2}\sin\omega t \quad (41)$$

where

$$F_{t1} = 2w'\omega\eta_2 v_2 + \lambda u_2,\ F_{t2} = -2w'\omega\eta_2 u_2 + \lambda v_2$$

Then, the amplitude, F_t of the dimensionless force, f_t transferred to the intermediate mass block is:

$$F_t = \sqrt{{F_{t1}}^2 + {F_{t2}}^2} \quad (42)$$

Similarly, the amplitudes of respective dimensionless speeds $\dot{z}_1$, $\dot{z}_2$ of the isolated equipment and the intermediate mass block are:

$$\dot{z}_{t1} = \sqrt{(-\omega u_1)^2 + (-\omega v_1)^2}$$
$$\dot{z}_{t2} = \sqrt{(-\omega u_2)^2 + (-\omega v_2)^2}$$

According to the definition of power transfer rates, the power transfer rate of the two-degree-of-freedom linear vibration isolation system is:

$$T_p = \frac{F_t\dot{z}_{t2}}{p\dot{z}_{t1}} = \frac{\sqrt{\left(2w'\omega\eta_2 v_2 + \lambda u_2\right)^2 + (-2w'\omega\eta_2 u_2 + \lambda v_2)^2}}{p\sqrt{(u_1^2 + v_1^2)/(u_2^2 + v_2^2)}} \quad (43)$$

2 Research on characteristics of power transfer rates

2.1 Influences of excitation amplitude on power transfer rates of system

Fig.4 shows power transfer rates of the double-layer vibration isolation system under different excitation-force amplitudes f in the case of fixed mass ratio, damping ratio, and stiffness ratio. According to Fig.4, the system has two orders of resonance peaks; the vibration corresponding to the first order resonance peak is dominated by the motion of the isolated equipment m_1, while the vibration corresponding to the second order peak is dominated by the motion of the intermediate mass block m_2; the same below. As the excitation-force amplitude increases, the second order resonance frequency remains unchanged, while the first order one increases, with the corre-

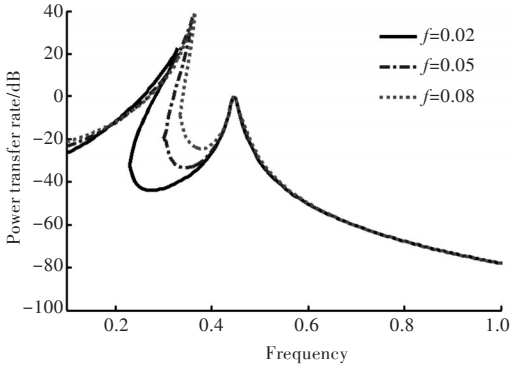

Fig.4 The reference values of power transfer rate of double layer vibration isolation system under different excitation force f

sponding power transfer rate increasing as well. In addition, the maximum power transfer rate corresponding to the second order resonance frequency is less than 1, indicating that the quasi-zero-stiffness vibration isolation system can still isolate vibration around its second order resonance frequency.

2.2 Influences of damping ratios on power transfer rates of system

Fig.5 shows power transfer rates of the double-layer vibration isolation system under different damping ratios ξ_1 (damping ratios of the springs in the quasi-zero-stiffness vibration isolator), in the case of fixed mass ratio, stiffness ratio and excitation-force amplitude. According to Fig.5, as the damping ratio ξ_1 increases, the second resonance frequency, as well as the power transfer rate corresponding to the first order resonance frequency, keeps unchanged, while the power transfer rate corresponding to the second order resonance frequency increases, indicating that vibration isolation performance of the vibration isolation system can be improved by reducing the damping ratio.

Fig.6 shows power transfer rates of the double-layer vibration isolation system under different damping ratios ξ_2 (damping ratios of the springs in the linear vibration isolator), in the case of fixed mass ratio, stiffness ratio and excitation-force amplitude. According to Fig.6, as the damping ratio increases, both the second order resonance frequency and its corresponding power transfer rate decrease. Therefore, vibration isolation performance of the vibration isolation system can be improved by reducing the damping ratio.

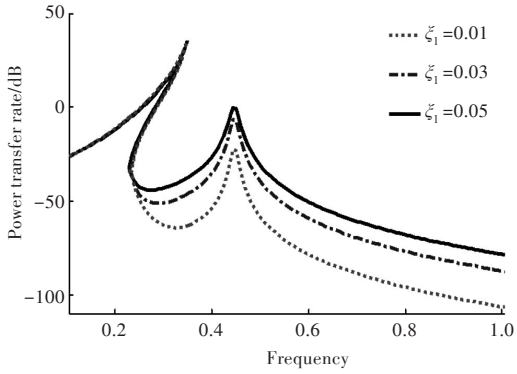

Fig.5 The reference values of power transfer rate of double layer vibration isolation system under different damping ratio ξ_1

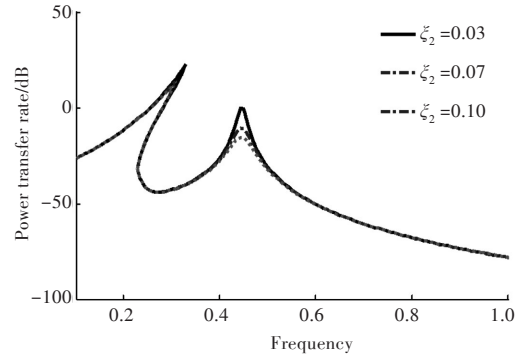

Fig.6 The reference values of power transfer rate of double layer vibration isolation system under different damping ratio ξ_2

2.3 Influences of mass ratios on power transfer rates of system

Fig.7 shows power transfer rates of the two-degree-of-freedom quasi-zero-stiffness vibration isolation system under different mass ratios w, in the case of fixed damping ratio, stiffness ratio and excitation-force amplitude. According to Fig.7, as the mass ratio increases, the maximum power transfer rate of the system and the first order resonance frequency basically remain unchanged, but the second order resonance frequency increases. Therefore, the mass ratio can be properly reduced to decrease the initial vibration isolation frequency of the system and increase its vibration isolation frequency range, so as to improve the low-frequency vibration isolation performance.

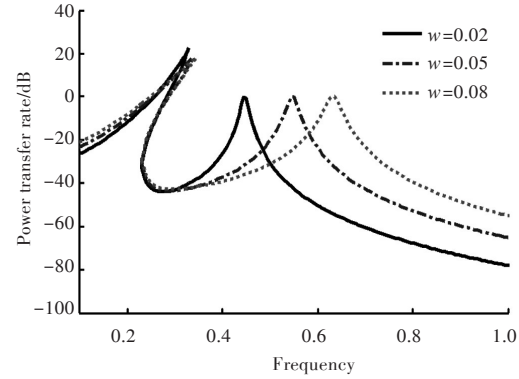

Fig.7 The reference values of power transfer rate of double layer vibration isolation system under different mass ratio w

2.4 Influences of stiffness ratios on power transfer rates of system

Fig.8 shows power transfer rates of the double-layer vibration isolation system under different stiffness ratios, in the case of fixed damping ratio, mass ratio and excitation-force amplitude. According to Fig.8, as the stiffness ratio β increases, both the first order resonance frequency and its corresponding power transfer rate of the system increase, while the second order resonance frequency and its corresponding power transfer rate remain unchanged. Therefore, vibration isolation performance of the quasi-zero-stiffness vibration isolation system can be improved by reducing the stiffness ratio properly.

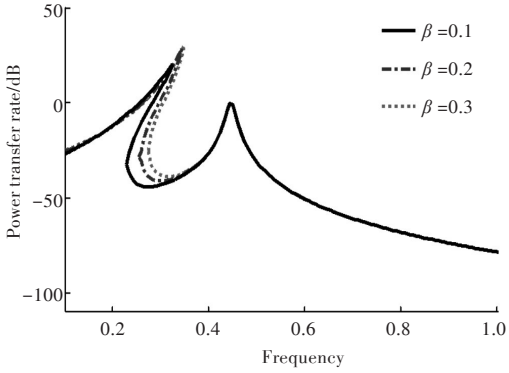

Fig.8 The reference values of power transfer rate of double layer vibration isolation system under different stiffness ratio β

3 Comparison between power transfer rates of the double-layer vibration isolation system and the two-degree-of-freedom linear vibration isolation system

In order to compare the performances of the double-layer vibration isolation system and the two-degree-of-freedom linear vibration isolation system, it is defined that the vertical spring with positive stiffness in the quasi-zero-stiffness vibration isolator has the same stiffness of k_1 as the linear vibration isolator does, to ensure the same bearing capacity of both isolators. In addition, it is defined that both systems have the same mass parameters m_1 and m_2, the same damping c_1 and c_2, the same stiffness k_2, and the same excitation $F\cos\Omega T$. According to dimensionless-parameter Formula (8) and Formula (25), damping ratios ξ_1 and ξ_2 and mass ratio w of the double-layer vibration isolation system are related to damping ratios η_1 and η_2 and mass ratio w' of the two-degree-of-freedom linear vibration isolation system in the following manner:

$$\eta_1=\frac{1}{2}\xi_1,\ \eta_2=\frac{1}{2}w\xi_2,\ w'=\frac{1}{w}$$

We take $\xi_1=0.05$, $\xi_2=0.05$, and $w=0.6$; accordingly, there are: $\eta_1=0.025$, $\eta_2=0.001\,5$, and $w'=5/3$. The excitation force of the equivalent linear vibration isolation system has no effect on the power transfer rate of the system, and the excitation force, p, is set to be 0.1.

According to Fig.9, compared with the two-degree-of-freedom equivalent linear vibration isolation system, the double-layer vibration isolation system has a lower initial vibration isolation frequency and a wider frequency range of vibration isolation, resulting in better performance in low-frequency vibration isolation. In addition, the maximum power transfer rate corresponding to the second order resonance frequency of the double-layer vibration isolation system is less than 1, indicating that the system is still workable to isolate vibration around the second order resonance frequency, so as to overcome shortcomings of the equivalent linear vibration isolation system.

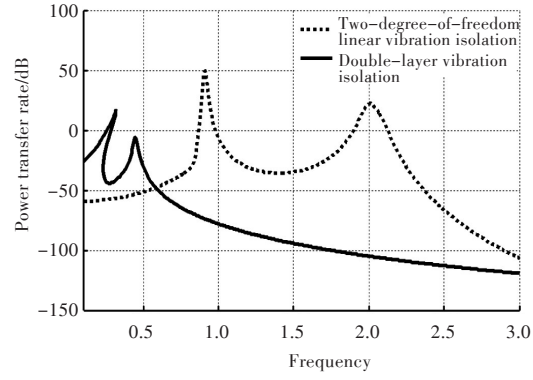

Fig.9 The reference values of power transfer rate of double layer vibration isolation system and equivalent linear vibration isolation system

4 Conclusion

In this paper, respective dynamic models of a double-layer vibration isolation system, composed of a linear vibration isolator and a quasi-zero-stiffness vibration isolator, and a linear vibration isolation system with two degrees of freedom have been established, and relevant power transfer rates have also been derived with the method of averaging. Following conclusions are obtained through comparative analysis of power transfer rates of the two systems:

1) vibration isolation performance of the double-layer vibration isolation system can be improved by properly reducing damping, mass, and stiffness ratios.

2) Compared with the two-degree-of-freedom equivalent linear vibration isolation system, the double-layer vibration isolation system has a lower initial vibration isolation frequency and a wider frequency range of vibration isolation, resulting in better performance in low-frequency vibration isolation.

3) The maximum power transfer rate corresponding to the second order resonance frequency of the double-layer vibration isolation system is less than 1, indicating that the system is still workable to isolate vibration around the second order resonance frequency, so as to overcome shortcomings of the two-degree-of-freedom linear vibration isolation system.

References

[1] ALABUZHEV P, GRITCHIN A, KIM L, et al. Vibration protecting and measuring systems with quasi-zero stiffness[M]. New York: CRC Press, 1989.

[2] XU D L, ZHANG Y Y, ZHOU J X, et al. Characteristic analysis and experimental investigation of a vibration isolator with quasi-zero-stiffness isolator[J]. Vibration and Shock, 2014, 33(11): 208-213 (in Chinese).

[3] ZHU S J, LOU J J, HE Q W, et al. Vibration theory and vibration isolation[M]. Beijing: National Defense Industry Press, 2006(in Chinese).

[4] WANG X L, ZHOU J X. Piecewise nonlinear-dynamic numerical analysis of a double-layer quasi-zero-stiffness vibration isolation system[C]// 2014 Proceedings of Chinese Conference on Computational Mechanics. Guiyang: Specialized Committee of Computational Mechanics from the Chinese Society of Theoretical and Applied Mechanics, 2014: 1-7(in Chinese).

[5] ZHOU J X, XU D L. Vibration isolation and chaotification of quasi-zero stiffness single- layer raft [J]. China Sciencepaper, 2014, 9(8): 911-915 (in Chinese).

[6] HUO R, SHI Y. The power flow efficiency criterion for vibration isolation design and its relationship with vibration level difference [J]. Shipbuilding of China, 2007, 48(3): 86-92 (in Chinese).

[7] LOU J J, LI C B, XIA J M, et al. Research on power flow transmission characteristics of flexible isolation system[J]. Ship Engineering, 2016, 38(7): 31-34 (in Chinese).

[8] XIA S C, HAN J S, HE L, et al. Power flow transmission of vibration isolating system on the flexible foundation[J]. Journal of Xi'an University of Science and Technology, 2007, 27(3): 419-422 (in Chinese).

[9] CARRELLA A, BRENMAN M J, WATERS T P. Static analysis of a passive vibration isolator with quasi-zero-stiffness characteristic[J]. Journal of Sound and Vibration, 2007, 301(3/4/5): 678-689.

[10] SUN H L, CHEN H B, ZHANG P Q, et al. Research on performance indices of vibration isolation system [J]. Applied Acoustics, 2008, 69(9): 789-795.

双层隔振系统隔振性能分析

赵建学[1], 俞翔[2], 柴凯[1], 杨庆超[2]

1 海军工程大学 动力工程学院, 武汉 430033

2 海军工程大学 科研部, 武汉 430033

摘　要: [**目的**] 研究准零刚度隔振器各系统参数对隔振性能的影响,可为其应用于隔振系统提供攻关方向。[**方法**] 以线性隔振、准零刚度隔振组成的双层隔振系统和两自由度等效线性隔振系统为对象,分别建立动力学模型;采用平均法推导谐波力激励条件下2个系统的功率流传递率,证明前者比后者有更好的隔振性能,并提出增强双层隔振系统隔振效果的方法。[**结果**] 研究表明,双层隔振系统第2阶共振频率对应的功率流传递率最大值小于1,意味着其在第2阶共振频率附近范围内仍具有隔振效果,从而克服了两自由度线性隔振系统的缺点。[**结论**] 双层隔振系统可通过适当减小阻尼比、质量比和刚度比来提高其隔振性能,且比等效线性隔振系统的低频隔振性能更好。

关键词: 准零刚度; 双层隔振; 功率流传递率